Zitierweise: *Angew. Chem. Int. Ed.* **2020**, *59*, 9542–9548
Internationale Ausgabe: doi.org/10.1002/anie.201916410
Deutsche Ausgabe: doi.org/10.1002/ange.201916410

Allyl Complexes

An η^3-Bound Allyl Ligand on Magnesium in a Mechanochemically Generated Mg/K Allyl Complex

*Ross F. Koby, Alicia M. Doerr, Nicholas R. Rightmire, Nathan D. Schley, Brian K. Long und Timothy P. Hanusa**

Abstract: *Milling two equivalents of K[1,3-$(SiMe_3)_2C_3H_3$] (= K[A′]) with MgX_2 (X = Cl, Br) produces the allyl complex $[K_2MgA'_4]$ (**1**). Crystals grown from toluene are of the solvated species $[(\eta^6\text{-tol})K)_2MgA'_4]$ ([**1**·2(tol)]), a trimetallic monomer with both bridging and terminal (η^1) allyl ligands. When recrystallized from hexanes, the unsolvated **1** forms a 2D coordination polymer, in which the Mg is surrounded by three allyl ligands. The C–C bond lengths differ by only 0.028 Å, indicating virtually complete electron delocalization. This is an unprecedented coordination mode for an allyl ligand bound to Mg. DFT calculations indicate that in isolation, an η^3-allyl configuration on Mg is energetically preferred over the η^1- (σ-bonded) arrangement, but the Mg must be in a low coordination environment for it to be experimentally realized. Methyl methacrylate is effectively polymerized by **1**, with activities that are comparable to K[A′] and greater than the homometallic magnesium complex $[\{MgA'_2\}_2]$.*

Introduction

Modern synthetic organic chemistry is inconceivable without organometallic compounds of the s-block metals, anchored by the development of the Grignard reagents (around 1900)[1] and alkyllithiums (1917).[2] Even though there have been spectacular advances that have addressed the limited covalency and metal-centered redox chemistry in Group 2 compounds,[3] ligand developments will probably remain the most direct way to work within the constraints of s-block electronic configurations, and these have led, for example, to dramatic developments in polymerization, hydrogenation, hydrosilylation, and hydroamination catalysts.[4] A particularly flexible basis for such ligand design is the allyl anion, $[C_3H_5]^-$, and its substituted derivatives. In combination with mechanochemical synthesis, we describe both a new coordination mode for the Mg-allyl bond and the catalytic reactivity of a heterometallic Mg/K-allyl complex, which demonstrate the still unexhausted variety and utility of the s-block-carbon bond.

The parent allyl ligand $[C_3H_5]^-$ is a sterically compact anion that is readily substituted to increase its size, and for associated complexes, their solubility and thermal stability.[5] The range of bonding modes documented for the allyl anion and its variants is remarkably large for such a small molecule: the commonly encountered terminal η^1- and η^3-conformations (along with various degrees of slippage) are accompanied with changes in π-electron delocalization (Figure 1 a–c). The bridging conformations of the allyl group are even more extensive, and at least six additional allyl–metal bonding modes have been structurally authenticated (Figure 1 d–i), although not all with a given metal.[6] However, for the Group 2 metals, only a limited range of bonding patterns has been documented. To date, beryllium compounds have been found with σ-bound (η^1) (Figure 1 a)[7] and μ_2-η^1,η^2 allyls (Figure 1 h).[8] In contrast, with very rare exceptions, η^3-conformations are uniformly the norm with complexes of the heavier alkaline-earth metals (Ca-Ba).[9] Magnesium represents a borderline case; explicit attempts to prepare magnesium species with η^3-bound allyls (Figure 1 b) have not been successful,[10] and at one time, based on the absence of any structural evidence to the contrary, σ-bonding was thought to be the preferred bonding mode for allyl ligands in magnesium compounds.[11] Later, a bridged μ_2-η^1,η^2 bonding mode was identified in a dimeric complex (Figure 2), and heterometallic potassium/magnesium species have been found that display additional complex bonding arrangements.[12] Without single-crystal X-ray data, structural confirmation of the Mg-allyl bond ligation mode is difficult, as allylmagnesium species are typically fluxional in solution, with NMR spectra that suggest the presence of trihapto-bound ligands. An example is provided by $[MgA'_2(thf)_2]$ (A′ = [1,3-$(SiMe_3)_2C_3H_3$]; Figure 2 a), which displays η^1-bound allyls in its crystal structure, but its solution NMR spectra give the appearance of more symmetrical, η^3-coordinated ligands; $\Delta G^{\ddagger}$ for the rearrange-

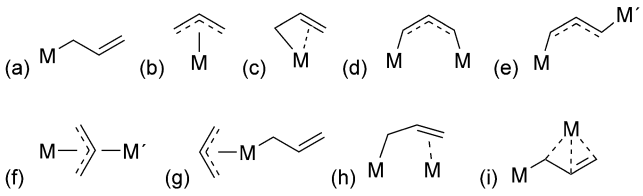

Figure 1. Some of the known bonding modes of the allyl ligand: a) η^1, b) η^3, c) η^1:η^2 d) *cis* μ_2-η^1:η^1, e) *trans* μ_2-η^1:η^1, f) μ_2-η^3:η^3, g) ($\eta^1+\eta^3$), h) μ_2-η^1:η^2, i) μ_2-η^1:η^3.

[*] R. F. Koby, N. R. Rightmire, N. D. Schley, Prof. T. P. Hanusa
Department of Chemistry, Vanderbilt University
Nashville, TN 37235 (USA)
E-Mail: t.hanusa@vanderbilt.edu
A. M. Doerr, Prof. B. K. Long
Department of Chemistry, University of Tennessee
Knoxville, TN 37996-1600 (USA)
E-Mail: long@utk.edu
Supporting information and the ORCID identification number(s) for the author(s) of this article can be found under: https://doi.org/10.1002/anie.201916410.

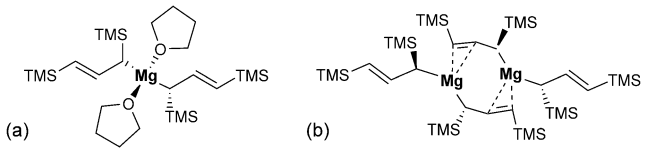

Figure 2. a) Connectivity of the solvated monomeric magnesium allyl $[MgA'_2(thf)_2]$ (A′ = [1,3-$(SiMe_3)_2C_3H_3$]); b) connectivity of the unsolvated dimeric magnesium allyl $[\{MgA'_2\}_2]$.

ment process is 12.3 kcal mol^{-1}.[13] Despite the lack of evidence in the solid state for η^3-bonded allyls on Mg, calculations have indicated that an unsolvated $[Mg(C_3H_5)_2]$ complex would have η^3-ligands,[13,14] and the occurrence of σ-bonding in known Mg-allyl compounds has been ascribed to the presence of coordinated solvents that cause a shift from η^3 to η^1 bonding.[13]

Apart from changing the bonding mode of allyl ligands, coordinated solvent can also affect reactions of the resultant complexes. The potentially depressant effect of such bases in Group 2 compounds was demonstrated by the ability of $[\{BDI^{Dipp}\}CaH]_2$ to insert non-activated α-olefins, generating $[\{BDI^{Dipp}\}CaR]_2$ calcium alkyl species, whereas the related $[\{BDI^{Dipp}\}CaH(thf)]_2$ is essentially inert.[15] Similarly, the solvated species $[MgA'_2(thf)_2]$ is inactive as an initiator for methyl methacrylate (MMA) polymerization, which is plausibly the result of the thf ligands hindering access to the metal center.[16] In contrast, preliminary tests (confirmed below) indicated that the unsolvated $[\{MgA'_2\}_2]$ dimer displays modest activity for MMA polymerization, a result that prompted us to explore the properties of the compound more completely.

The strength of the Mg-thf interaction is such that $[MgA'_2(thf)_2]$ cannot be directly desolvated, and to obtain the solvent-free material the diethyl ether adduct $[MgA'_2(Et_2O)_2]$ must first be prepared and the ether subsequently removed under high vacuum.[13] In an attempt to simplify the process and avoid the use of coordinating solvents, we turned to mechanochemistry, the use of mechanical force or energy to drive reactions.

Mechanochemical synthesis can yield unique products that cannot be prepared from solution-based approaches. In recent years, mechanochemically induced reactions have become more widely employed, although compared to the progress in organic[17] and materials chemistry, that in organometallic synthesis is more limited.[17b,18] In particular, the consequences of removing the solvent from the reaction environment are not yet readily predictable. Some syntheses are solvent-indifferent (for example, that for ferrocene[19]), or at least generate the product expected from the stoichiometry of the reagents (for example, the formation of $[AlA'_3]$ from the mixture of $AlI_3 + 3$ K[A′][20]). However, non-stoichiometric outcomes are also common (such as the formation of the stannate $K[SnA'_3]$ from a 1:2 reaction of $SnCl_2$ and K[A′],[21] or the formation of $K[Ca\{N(TMS)_2\}_3]$ from 1:2 reaction of CaI_2 and $K[N(TMS)_2]$.[22] In these cases, the unexpected complexes appear to be non-equilibrium products, formed too rapidly from the high concentration of reactants in the solid state for the equilibrium stoichiometry to be established.

Results and Discussion

Even though the possibility certainly existed that something other than the desired $[\{MgA'_2\}_2]$ would be produced on grinding, MgX_2 (X = Cl or Br) was milled with two equivalents of K[A′] for 10–15 min at 600 rpm in a planetary mill. Extraction of the resulting pale-orange solid with hexanes (neither of the starting materials is hexanes-soluble), filtration of the extract, and removal of solvent from the filtrate left an orange oil. The oil produced highly air- and moisture-sensitive microcrystals (**1**) on standing overnight. ^{1}H NMR spectra display a splitting pattern of 2 triplets, 2 doublets, and 2 singlets, corresponding to a set of two distinct A′ ligands that are in a 2:1 ratio by integration of peak area.[23] These resonances are clearly different from those in the more complex spectrum of $[\{MgA'_2\}_2]$, which reflect monomer-⇄dimer rearrangement in solution.[7]

Crystals of **1** suitable for X-ray crystal diffraction were originally grown from a slowly evaporated toluene solution, and although they ultimately yielded a structure of connectivity-only quality (Figure 3), several features are worth

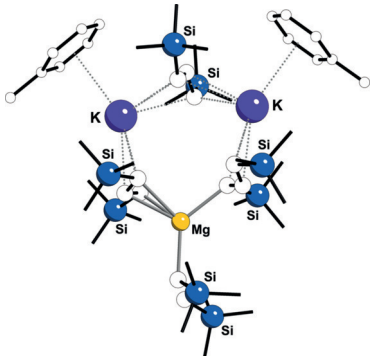

Figure 3. Connectivity-only structure of $[((\eta^6\text{-tol})K)_2MgA'_4]$ ([**1**·2(tol)]). For clarity, disorder in a toluene and in the $SiMe_3$ groups is not shown, and all hydrogen atoms have been removed, as have the carbon atoms in the $SiMe_3$ groups.

noting. The complex is a trimetallic monomer with a fundamental composition of 2:1:4 K/Mg/A′, which does not reflect the reagent stoichiometry. One allyl ligand is found η^1-bonded to the Mg center. The other three are bridging, either between the potassium atoms, each of which is capped with a π-bound toluene ligand, or between the magnesium and the potassium atoms. Unfortunately, owing to disorder in almost all of the trimethylsilyl groups and in one of the toluenes, the quality of structure prevents further discussion of the bonding.

Higher-quality crystals of [**1**·2(tol)] could not be obtained with slow evaporation, but recrystallization from hexanes was successful, leading to a structure free from disorder. Single-crystal X-ray diffraction revealed that the 2:1:4 K/Mg/A′ composition of the toluene solvate is maintained, but the unsolvated **1** now forms a 2D coordination polymer (Figures 4, 5), which is isostructural with the Mn^{II} analogue.[24] Two of the allyl ligands on the Mg cation are η^1-bonded and the third (C1–C3) is η^3-bonded. Both of the allyls that are η^1-coordinated to Mg are π-bonded to potassium cations,

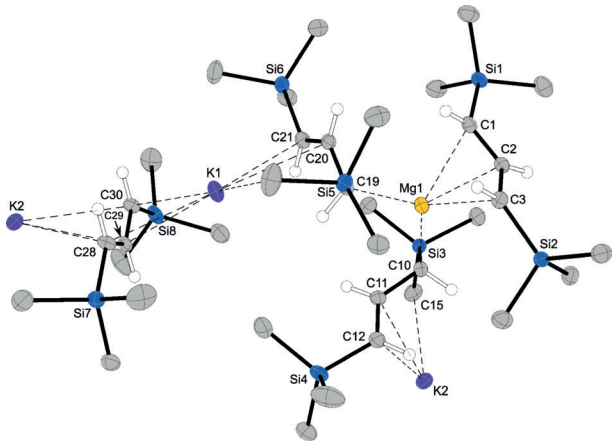

Figure 4. Plot () of a portion of the coordination polymer of $\{[K_2MgA'_4]\}_n$ (**1**).[42] Ellipsoids are set at 50% probability; for clarity, hydrogen atoms have been removed from trimethylsilyl groups. Selected bond distances and angles: Mg1–C19 2.206(3) Å, Mg1–C10 2.235(4) Å, Mg1–C1 2.446(4) Å, Mg1–C2 2.338(4) Å, Mg1–C3 2.375(4) Å, C1–C2 1.389(5) Å, C2–C3 1.417(4) Å, K1–C21 2.997(3) Å, K1–C20 3.206(3) Å, K1···C19 3.407(3) Å, K1–C28 3.104 Å, K1–C29 2.929 Å, K1–C30 3.002 Å, K2–C11 3.133(4) Å, K2–C12 3.057(4) Å, K1···C10 3.319(4) Å; C1-C2-C3 128.9(3)°.

extending the polymer in a sheet in the *ab* plane; the η^3-allyl ligand is terminal. Each of the potassium atoms is coordinated to an additional K[A′] before the chain continues with a Mg core. There are two independent polymer systems in the asymmetric unit. Potassium coordination spheres are completed with methyl groups from symmetry-equivalent polymers, (K···CH_3 3.34 Å), and every other layer repeats along the *c*-axis (Figure 5).

There are two crystallographically independent, but similar, magnesium centers, and only the coordination environment around Mg1 will be discussed here. The two Mg–C bonds to the η^1-bonded allyls are 2.206(3) and 2.235(4) Å, similar to that in $[MgA'_2(thf)_2]$ (2.197(3) Å). The η^3-bonded allyl is the first structurally authenticated example of

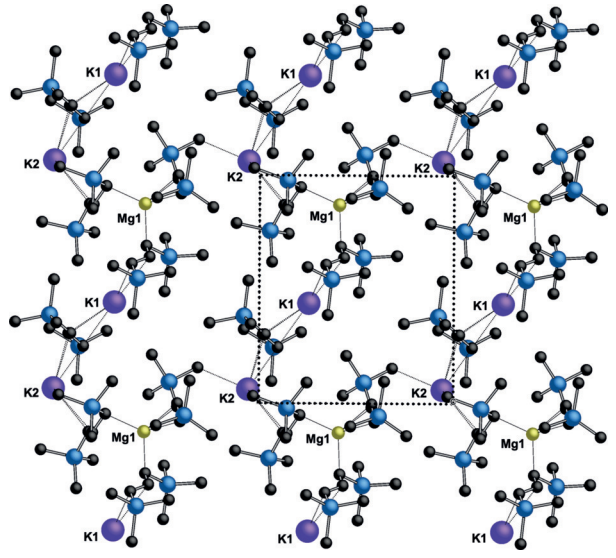

Figure 5. Partial packing diagram of $\{K_2[MgA'_4]\}_n$ (the *c* axis is vertical). Hydrogen atoms are omitted for clarity.

such a fragment, as it is both terminal (not bridging as in $[\{MgA'_2\}_2]$) and the C–C bonds in the allyl unit differ by only 0.028 Å, indicating virtually complete electron delocalization in the anion. It is somewhat slipped from symmetrical coordination, with terminal Mg–C bond lengths of 2.375(4) and 2.446(4) Å. Such slippage is common in systems with highly polar metal–allyl bonding.[25]

The bonding of the allyl ligands to the potassiums is irregular; K2 is η^2-bonded to the [C10-C12] allyl at an average distance of 3.10 Å (to C11/C12; the K1···C10 contact is at 3.32 Å). K2 also displays a contact at 3.09 Å to the methyl group C15 on Si3 (the K···H(C) distance is 2.60 Å, which is probably energetically significant). The allyl bridging between K1 and K2 (C28–C30) is fully delocalized ($\Delta_{C\text{-}C}$ = 0.004 Å), and displays μ_2-η^3:η^3 bonding to the potassium atoms, with average K–C distances of 3.050 Å (to K2) and 3.012 Å (to K1). The range of distances is similar to that observed in the coordination polymers $[\{K[A']\}_\infty]$ and $[\{K[A'](thf)_{3/2}\}_\infty]$.[26]

Polymerization Results

Metal (trimethylsilyl)allyl complexes have been previously evaluated as initiators for the polymerization of MMA.[16,27] Consequently, the MMA polymerization activity of **1** was evaluated and compared to the activities of the $[\{MgA'_2\}_2]$ complex and the previously reported K[A′].[27b] All polymerizations were conducted under an inert atmosphere in which the initiator, MMA (0.5 g), and toluene (2 M) were combined and allowed to react at the designated temperature and time, as detailed in Table 1. Room-temperature polymerizations using initiators K[A′], **1**, and $[\{MgA'_2\}_2]$ and a high monomer/initiator loading (100:1) were found to reach 94%, 72%, and 19% yield, respectively, in 24 h (Table 1, entries 1–3). These results are consistent with the hypothesis that the polymerization inactivity of previously reported $[MgA'_2(thf)_2]$ species is due in part to solvent coordination, thereby hindering monomer coordination to the metal center.[16]

When comparing the polymers produced using K[A′], **1**, and $[\{MgA'_2\}_2]$, we found that initiators K[A′] and **1** both produce atactic poly(methylmethacrylate) (PMMA) with similar molecular weights (M_n) and dispersities ($Đ$). In contrast, $[\{MgA'_2\}_2]$ produced isotactically enriched PMMA having a significantly higher M_n and a broader dispersity ($Đ$ = 3.83; Table 1, entry 3). To further investigate the activity of catalyst **1**, MMA polymerizations were conducted at lower initiator loading (250:1) and shorter polymerization time (1 h). Again, initiators K[A′] and **1** exhibited similar activities reaching 90% and 72% yield, respectively (Table 1, entries 4, 5), indicating that polymerizations using these initiators are rapid and reach their maximum possible conversion in ≤1 h. However, $[\{MgA'_2\}_2]$ exhibited dramatically decreased activity, only producing trace amounts of polymer under identical conditions (Table 1, entry 6).

Lastly, the catalytic activity of **1** was examined for MMA polymerizations at 0°C and a further decreased initiator loading of 1000:1 (MMA:**1**). K[A′] again exhibited similar activity reaching 92% in 1 h (Table 1, entry 7), whereas

Tabelle 1: Polymerization of MMA with initiator K[A′], $[K_2MgA'_4]$ (**1**), and $[\{MgA'_2\}_2]$.[a]

Entry	Initiator	Mono/init	T [°C]	t [h]	Yield[b] [%]	M_n[c] [g mol^{-1}]	M_w/M_n	Tacticity[d]
1	K[A′]	100:1	RT	24	94	19100	2.68	26/50/24 (atactic)
2	$[K_2MgA'_4]$ (**1**)	100:1	RT	24	72	17800	2.76	25/52/23 (atactic)
3	$[\{MgA'_2\}_2]$	100:1	RT	24	19	113400	3.83	71/16/12 (isotactic enriched)
4	K[A′]	250:1	RT	1	90	25500	2.37	–
5	$[K_2MgA'_4]$ (**1**)	250:1	RT	1	72	20500	2.18	–
6	$[\{MgA'_2\}_2]$	250:1	RT	1	trace	–	–	–
7	K[A′]	1000:1	0	1	92	46900	2.62	–
8	$[K_2MgA'_4]$ (**1**)	1000:1	0	1	89	27800	2.89	–
9	$[\{MgA'_2\}_2]$	1000:1	0	1	0	–	–	–

[a] General conditions: 0.5 g monomer, 2 M in toluene, quenched with MeOH. [b] Yield was determined based upon isolated polymer mass and initial mass of MMA. [c] Determined using gel permeation chromatography at 40 °C in THF and are reported relative to a PMMA standard. [d] Determined with ^{1}H NMR in $CDCl_3$ by integrating the methyl region.

initiator **1** exhibited an increase in activity at this lower polymerization temperature, ultimately reaching 89% conversion in 1 h (Table 1, entry 8). Though the source of this increase in activity is not yet fully understood, we hypothesize that this may indicate that initiator **1** undergoes decomposition and/or deactivation at room temperature, which is slowed or suppressed at temperatures at or below 0 °C.[28] Finally, and as expected at this point, $[\{MgA'_2\}_2]$ exhibited no polymerization activity under these conditions (Table 1, entry 9).

Computational Results

Isolated complexes involving the A′ ligand and a monovalent/ divalent metal combination have to date been of the form $[M^IM^{II}A'_3]$, where three allyl ligands are bound to the M^{II} metal in a C_3-symmetric *tris*-(η^1) fashion and sequester an $[M^I]^+$ cation in the *ansa*-tris(η^2-olefin) pocket through a cation–π interaction (for example, Figure 6); such interaction is calculated to contribute as much as 24 kcal mol^{-1} to the stability of the compound when $M^I = K$.[29] The range of M^{II} ions that have been incorporated into structurally characterized compounds includes Zn (for which combinations with M^I = Li, Na, and K are known), Be,[8] and Sn.[21,30] It seemed unusual that this was not the form of the metalate adopted by the Mg derivative, especially as the ionic radii of Mg^{2+} and Zn^{2+}, for example, are similar (0.57 Å and 0.60 Å, respectively, for CN = 4).[31] The electronegativity of Mg (1.31, Pauling scale[32]) is less than any of other divalent metals used to date (1.57, 1.65, and 1.80 for Be, Zn, and Sn, respectively), however, and the Mg–C bond is somewhat more polar than the other M–C cases. The effect that this might have on the relative stability of η^3- over η^1- bonding was examined with a DFT computational investigation (B3PW91-D3BJ/def2TZVP) of a selected set of $[M^{II}A'_2]$ and $[KM^{II}A'_3]$ (M^{II} = Be, Mg, Zn, Sn) complexes (for details see the Supporting Information). In the optimized $[MA'_2]$ complexes, Zn and Sn have η^1-bound allyls, indicating a preference that is corroborated by the lack of any structurally authenticated η^3-bound allyls on Zn,[33] though some have recently been identified for Sn.[34] For the more electropositive elements (Be, Mg), $[M(\eta^3\text{-}A')_2]$ geometries are lower in energy than the $[M(\eta^1\text{-}A')_2]$ counterparts; the preference for η^3- over η^1- in the case of Be is small (4.4 kcal mol^{-1}), but it doubles to 9.0 kcal mol^{-1} for Mg.[35]

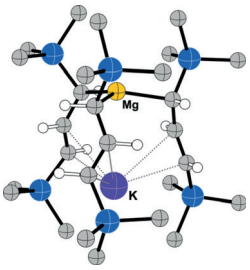

Figure 6. Calculated structure (B3PW91-D3BJ/def2TZVP) of $[Mg(\mu_2\text{-}\eta^1,\eta^2\text{-}A')_3K]$ (C_3 symmetry, H atoms omitted from the TMS groups). Mg–C 2.178 Å; C_α–C_β 1.441 Å; C_β–C_γ 1.364 Å; K···C = 2.93, 3.23 Å; sum of C-Mg-C′ 354.4°.

Calculations on the monomeric $[KM^{II}A'_3]$ complexes indicated that all of them were at least local minima on their respective potential energy surfaces. The reason that a monomeric $[KMg(\eta^1\text{-}A')_3]$ complex is not isolated may be largely a result of the preference of magnesium for η^3- over η^1-allyl bonding. Furthermore, the polymeric structure of **1** provides for an η^3- interaction of the allyls with K^+, which should provide greater stabilization than that from the η^2 cation–π interactions with the C=C double bonds in a $[KMg(\eta^1\text{-}A')_3]$ complex.[36] Finally, issues of coordinative (un)saturation at the metal center may be in play. With the program Solid-G,[37] the net percentage of coordination sphere covered by the ligands in a complex may be estimated as the $G_{complex}$ value (Figure 7). The value for the hypothetical $[MgA'_2]$ is 79.0% (7a), but in the solvated $[MgA'_2(thf)_2]$ complex, it increases to 89.8% (see the Supporting Information). A similar number (93.0%) is calculated for the $[\{MgA'_2\}_2]$ dimer (7b), and also for the Mg supporting the η^3-A′ ligand in **1** (that is, in the $[K_2MgA'_3]^+$ fragment, at 90.1%, 7c).[38] The $G_{complex}$ value for the 3 allyl ligands around Mg in monomeric $[KMg(\eta^1\text{-}A')_3]$ is 84.9% (7d), roughly halfway between the values for the exposed $[MgA'_2]$ and the enclosure in **1**. This suggests that an undersaturated Mg center may boost its coverage by whatever means are at hand: if THF or Et_2O molecules are available, it will coordinate to them, but if not, the complex will dimerize. Alternatively, the presence of extra K[A′] in the same phase provides an opportunity for metal coordination through the formation of a coordination polymer, which

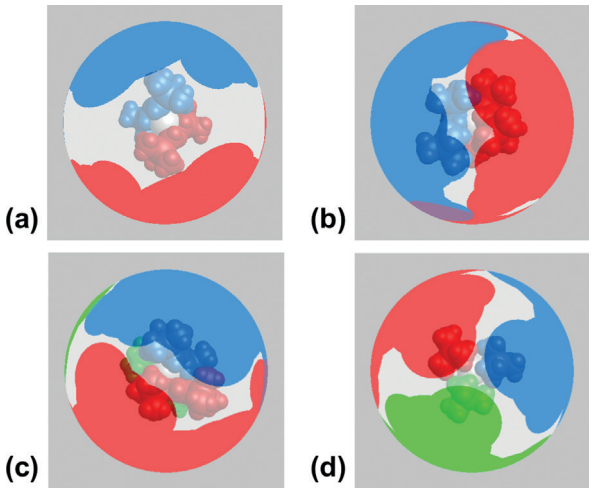

Figure 7. Visualization of the extent of coordination sphere coverage ($G_{complex}$) of: a) [MgA′$_2$], 79.0%; b) [{MgA′$_2$}$_2$], (C_2 symmetry), 93.0%; c) [K_2MgA′$_3$]$^+$ (fragment derived from **1**), 90.1%; d) [MgA′$_3$] fragment, from the hypothetical [KMg(η^1-A′)$_3$] (C_3 symmetry, Mg at the center, K removed), 84.9%. Optimized coordinates (B3PW91-D3BJ/def2-TZVP) and the program Solid-G were used. The $G_{complex}$ value represents the net coverage, so that regions of the coordination sphere where the projections of the ligands overlap are counted only once.

provides better metal saturation than the monomeric [KMg(η^1-A′)$_3$].

Requirements for Trihapto Allyl Bonding to Mg

The long-standing difficulty of isolating a compound with an η^3-allyl ligand on Mg seems to conflict with computational evidence suggesting that such a bonding mode should be preferred over an η^1-bonded arrangement. An earlier DFT investigation indicated that the addition of THF to [Mg(η^3-C_3H_5)$_2$] caused successive slippage of the allyl ligands to [Mg(η^3-C_3H_5)(η^1-C_3H_5)(thf)] and then to [Mg(η^1-C_3H_5)$_2$(thf)$_2$].[13] The exact reason for the slippage, whether primarily steric, electronic, or a combination of the two, was left unresolved. That a relatively crowded coordination sphere coverage of 90% (Figure 7c) is still compatible with an η^3-A′ ligand, however, indicates that slippage of the ligand should not be uncritically ascribed to simple steric effects.

In the allyl anion, the negative charge is concentrated on the terminal carbons.[39] This fact, combined with the calculated [Mg(η^3-C_3H_5)$_2$]→[Mg(η^3-C_3H_5)(η^1-C_3H_5)(thf)]→[Mg(η^1-C_3H_5)$_2$(thf)$_2$] progression noted above, suggests that the change in allyl hapticity occurs to maintain a roughly tetrahedral distribution of charge around the Mg. The relevance of these results to the structurally authenticated **1** can be appreciated by viewing the η^3-bound allyl from a point almost perpendicular to the C_3 plane (Figure 8). The most negatively charged carbons surrounding the Mg are C1/C3 of the π-bound allyl, and C10 and C19 of the neighboring σ-bonded allyls, which are at similar distances to Mg (2.23 and 2.21 Å, respectively). The angle between the planes defined by C1/Mg/C3 and C10/Mg/C19 is 77.0°.

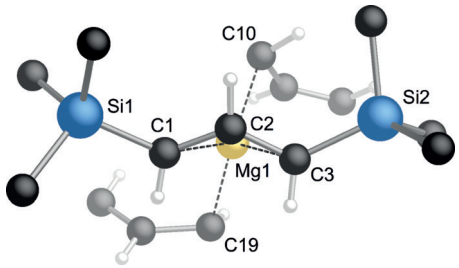

Figure 8. A fragment of the structure of **1**, viewed almost perpendicularly to the η^3-allyl C_3 plane; hydrogens have been removed from the TMS groups. The angle between the planes defined by C1/Mg/C3 and C10/Mg/C19 is 77.0°. The analogous angle calculated for the unsubstituted [$MgK_2(C_3H_5)_3$]$^+$ cation is 87.0°.

These tetrahedral or pseudo-tetrahedral geometries are related to the unique set of properties magnesium brings to an organometallic complex. The polarity of the Mg–C bond is moderately high, but the electropositivity of Mg is not enough to support the η^3-bonding expected from an essentially ionic interaction, that is, as a $[Mg]^{2+}[C_3H_5]^-$ ion pair, as observed with the alkali metals or heavier Group 2 metals. An orbitally supported η^3-allyl configuration, relying on a formally sp^3-hybridized Mg center, will engage two of the four available orbitals, leaving only two to bind to additional ligands. The tetrahedral arrangement of bonding associated with an η^3-allyl ligand is apparent in a Bader analysis (atoms in molecules, AIM) of [Mg(C_3H_5)$_2$] and the [K_2Mg(C_3H_5)$_3$]$^+$ cation (Figure 9). The bond critical paths (BCP) connect the

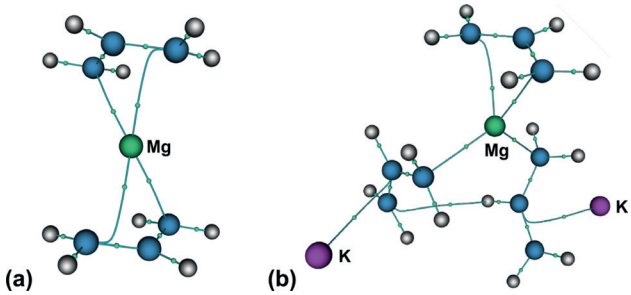

Figure 9. Bond critical points (dots) and bond paths (lines) obtained from AIM calculations for: a) the neutral [Mg(C_3H_5)$_2$] complex; b) the [K_2Mg(C_3H_5)$_3$]$^+$ cation. The average electron density of the bond critical points from Mg to the terminal carbons of the allyls in [Mg(C_3H_5)$_2$] is 0.037 e^-Å^{-3}; that to the terminal carbons of the η^3-bound allyl in [K_2Mg(C_3H_5)$_3$]$^+$ is 0.034 e^-Å^{-3}, and to the terminal carbons of the η^1-bound allyls is 0.040 e^-Å^{-3}.

most negative centers in the allyl anions to the Mg centers, whereas in the cation, a single BCP is observed between K^+ and the closest carbon atom of the adjacent allyl, a bonding pattern found before with highly ionic interactions.[40] A more detailed contour mapping of the Mg–allyl interaction in the [K_2Mg(C_3H_5)$_3$]$^+$ cation is available in the Supporting Information.

A survey of the Cambridge Structural Database reveals that all structurally authenticated magnesium compounds with one or more terminal allyl ligands (all σ-bonded) are at least 4-coordinate (see the Supporting Information), which

means that if an allyl ligand were to shift to a permanent η^3-configuration, the effective coordination number would rise to at least 5 or greater. Without the electropositive character of the metal or sufficient orbitals to support η^3-allyl bonding under such conditions, the allyl will remain σ-bonded. An illustration of this situation is provided by the PMDTA adducts of lithium and magnesium allyl complexes, established crystallographically as $[Li(\eta^3\text{-}C_3H_5)(PMDTA)]$[25] and $[Mg(\eta^1\text{-}C_3H_5)(PMDTA)(thf)]^+[B(C_6F_5)_4]^-$.[12] To make the coordination environments equivalent and to remove any effects of crystal packing, the geometries of the neutral $[Li(C_3H_5)(PMDTA)]$ and cationic $[Mg(C_3H_5)(PMDTA)]^+$ cation complexes were optimized at the B3PW91-D3BJ/def2TZVP level. The allyl ligand remains η^3-allyl bound to Li, and η^1-bound to Mg (Figure 10), consistent with the analysis above.

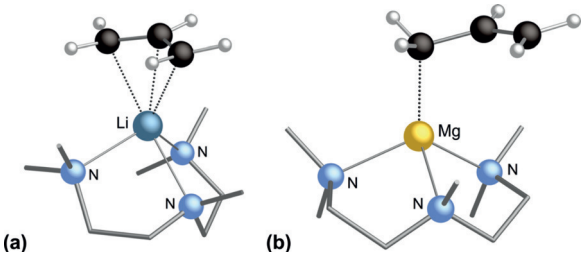

Figure 10. Geometry-optimized structures of a) $[Li(\eta^3\text{-}C_3H_5)(PMDTA)]$ and b) $[Mg(\eta^1\text{-}C_3H_5)(PMDTA)]^+$. The Li–C bonds average to 2.24 Å, and the allyl C–C bonds differ by 0.002 Å. The Mg-C_α distance is 2.112 Å, whereas the other carbons are > 2.8 Å away. The allyl C–C bond lengths differ by 0.147 Å.

Conclusion

We have prepared through mechanochemical synthesis the first compound containing a structurally authenticated η^3-bound allyl ligand on a magnesium center. The rarity of this particular bonding mode appears to stem from a combination of properties particular to magnesium, specifically its intermediate electropositivity and limited set of valence orbitals. To realize the trihapto bonding, a relatively low coordination number for the metal is required, which can be summarized for a monometallic complex with the formula $[(\eta^3\text{-allyl})_xMgX_yL_z]^{2-(x+y)}$ (X is a monoanion; L is a neutral donor) by the relationship $2x + y + z \leq 4$. Consequently, if $x = 2$ (two η^3-allyls), y and z can only be zero, as predicted for the structure of $[Mg(\eta^3\text{-allyl})_2]$. Similarly, if one adds a neutral donor to $[Mg(\eta^3\text{-allyl})_2]$, only one of the allyls can remain η^3-bound, as calculated for $[Mg(\eta^3\text{-}C_3H_5)(\eta^1\text{-}C_3H_5)(thf)]$. The presence of the η^3-A′ ligand in **1** follows from the values $x = 1$, $y = 2$, corresponding to the $[(\eta^3\text{-A}')Mg(\eta^1\text{-A}')_2]^-$ anionic fragment. The isolation of **1** was aided by the bulk of the A′ ligand, which discourages additional coordination, and by the solvent-free mechanochemical synthesis, but there is no reason why this unusual bonding mode could not be recreated in other organomagnesium compounds.

The polymerization of MMA by K[A′], **1**, and $[\{MgA'_2\}_2]$ demonstrates the influence of the metal identity on polymerization activity. $[\{MgA'_2\}_2]$ is certainly the least active of the three, but does provide some measure of stereocontrol, as evidenced by the enhanced isotacticity of the PMMA produced. K[A′] is by far the most active, and is effective at 1000:1 loading, but produces atatic polymer. The polymerization behavior of **1** appears to be influenced by its preponderance of potassium, in that its activity is far higher than that of $[\{MgA'_2\}_2]$, and approaches that of K[A′], and it has also lost any stereocontrol over polymerization, generating only atactic polymer. There has been growing interest in studying the properties of heterometallic main-group systems in both stoichiometric and catalytic contexts,[12,41] and the ability to generate new classes of such compounds mechanochemically suggests that expanded investigations of heterometallic reactivity will be possible.

Acknowledgements

Financial support by the National Science Foundation (CHE-1665327), ACS-PRF (56027-ND3), and a Charles M. Lukehart Fellowship (to R.F.K.) is gratefully acknowledged. Professor Arnold L. Rheingold is thanked for providing the structure of [**1**·2(tol)].

Conflict of interest

The authors declare no conflict of interest.

Stichwörter: allyl · magnesium · mechanochemistry · polymerization · potassium

[1] a) V. Grignard, *C. R. Hebd. Seances Acad. Sci.* **1900**, *130*, 1322–1324; b) V. Grignard, *C. R. Hebd. Seances Acad. Sci.* **1901**, *132*, 558–561; c) V. Grignard, *Ann. Chim.* **1901**, *24*, 433–490; d) D. S. Ziegler, B. Wei, P. Knochel, *Chem. Eur. J.* **2019**, *25*, 2695–2703.
[2] a) W. Schlenk, J. Holtz, *Ber. Dtsch. Chem. Ges.* **1917**, *50*, 262–274; b) U. Wietelmann, J. Klett, *Z. Anorg. Allg. Chem.* **2018**, *644*, 194–204.
[3] a) S. Krieck, H. Görls, L. Yu, M. Reiher, M. Westerhausen, *J. Am. Chem. Soc.* **2009**, *131*, 2977–2985; b) S. P. Green, C. Jones, A. Stasch, *Angew. Chem. Int. Ed.* **2008**, *47*, 9079–9083; *Angew. Chem.* **2008**, *120*, 9219–9223; c) S. J. Bonyhady, C. Jones, S. Nembenna, A. Stasch, A. J. Edwards, G. J. McIntyre, *Chem. Eur. J.* **2010**, *16*, 938–955; d) J. Overgaard, C. Jones, A. Stasch, B. B. Iversen, *J. Am. Chem. Soc.* **2009**, *131*, 4208–4209.
[4] a) J. Spielmann, F. Buch, S. Harder, *Angew. Chem. Int. Ed.* **2008**, *47*, 9434–9438; *Angew. Chem.* **2008**, *120*, 9576–9580; b) J. Spielmann, S. Harder, *Eur. J. Inorg. Chem.* **2008**, 1480–1486; c) S. Harder, *Chem. Rev.* **2010**, *110*, 3852–3876; d) H. Bauer, M. Alonso, C. Färber, H. Elsen, J. Pahl, A. Causero, G. Ballmann, F. De Proft, S. Harder, *Nat. Catal.* **2018**, *1*, 40–47; e) H. Bauer, M. Alonso, C. Fischer, B. Roesch, H. Elsen, S. Harder, *Angew. Chem. Int. Ed.* **2018**, *57*, 15177–15182; *Angew. Chem.* **2018**, *130*, 15397–15402.
[5] a) S. C. Chmely, T. P. Hanusa, *Eur. J. Inorg. Chem.* **2010**, 1321–1337; b) S. A. Solomon, R. A. Layfield, *Dalton Trans.* **2010**, *39*, 2469–2483.
[6] C. Lichtenberg, J. Okuda, *Angew. Chem. Int. Ed.* **2013**, *52*, 5228–5246; *Angew. Chem.* **2013**, *125*, 5336–5354.

[7] S. C. Chmely, T. P. Hanusa, W. W. Brennessel, *Angew. Chem. Int. Ed.* **2010**, *49*, 5870 – 5874; *Angew. Chem.* **2010**, *122*, 6006 – 6010.
[8] N. Boyde, N. Rightmire, T. Hanusa, W. Brennessel, *Inorganics* **2017**, *5*, 36.
[9] a) P. Jochmann, T. P. Spaniol, S. C. Chmely, T. P. Hanusa, J. Okuda, *Organometallics* **2011**, *30*, 5291 – 5296; b) C. Lichtenberg, P. Jochmann, T. P. Spaniol, J. Okuda, *Angew. Chem. Int. Ed.* **2011**, *50*, 5753 – 5756; *Angew. Chem.* **2011**, *123*, 5872 – 5875; c) P. Jochmann, J. P. Davin, S. Maslek, T. P. Spaniol, Y. Sarazin, J.-F. Carpentier, J. Okuda, *Dalton Trans.* **2012**, *41*, 9176 – 9181.
[10] P. J. Bailey, S. T. Liddle, C. A. Morrison, S. Parsons, *Angew. Chem. Int. Ed.* **2001**, *40*, 4463 – 4466; *Angew. Chem.* **2001**, *113*, 4595 – 4598.
[11] S. A. Solomon, C. A. Muryn, R. A. Layfield, *Chem. Commun.* **2008**, 3142 – 3144.
[12] C. Lichtenberg, T. P. Spaniol, I. Peckermann, T. P. Hanusa, J. Okuda, *J. Am. Chem. Soc.* **2013**, *135*, 811 – 821.
[13] S. C. Chmely, C. N. Carlson, T. P. Hanusa, A. L. Rheingold, *J. Am. Chem. Soc.* **2009**, *131*, 6344 – 6345.
[14] K. Walczak, J. Friedrich, M. Dolg, *Chem. Phys.* **2010**, *376*, 36 – 45.
[15] a) A. S. S. Wilson, C. Dinoi, M. S. Hill, M. F. Mahon, L. Maron, *Angew. Chem. Int. Ed.* **2018**, *57*, 15500 – 15504; *Angew. Chem.* **2018**, *130*, 15726 – 15730; b) A. S. S. Wilson, M. S. Hill, M. F. Mahon, C. Dinoi, L. Maron, *Science* **2017**, *358*, 1168 – 1171.
[16] K. T. Quisenberry, R. E. White, T. P. Hanusa, W. W. Brennessel, *New J. Chem.* **2010**, *34*, 1579 – 1584.
[17] a) D. Tan, L. Loots, T. Friščić, *Chem. Commun.* **2016**, *52*, 7760 – 7781; b) J. G. Hernández, C. Bolm, *J. Org. Chem.* **2017**, *82*, 4007 – 4019; c) J. Andersen, J. Mack, *Green Chem.* **2018**, *20*, 1435 – 1443; d) J. L. Howard, Q. Cao, D. L. Browne, *Chem. Sci.* **2018**, *9*, 3080 – 3094; e) T. Friščić, C. Mottillo, H. M. Titi, *Angew. Chem. Int. Ed.* **2020**, *59*, 1018 – 1029.
[18] a) N. R. Rightmire, T. P. Hanusa, *Dalton Trans.* **2016**, *45*, 2352 – 2362; b) A. A. Gečiauskaitė, F. García, *Beilstein J. Org. Chem.* **2017**, *13*, 2068 – 2077; c) D. Tan, F. García, *Chem. Soc. Rev.* **2019**, *48*, 2274 – 2292; d) J. G. Hernández, C. Bolm, *Chem. Commun.* **2015**, *51*, 12582 – 12584; e) K. Budny-Godlewski, I. Justyniak, M. K. Leszczyński, J. Lewiński, *Chem. Sci.* **2019**, *10*, 7149 – 7155.
[19] V. D. Makhaev, A. P. Borisov, L. A. Petrova, *J. Organomet. Chem.* **1999**, *590*, 222 – 226.
[20] N. R. Rightmire, T. P. Hanusa, A. L. Rheingold, *Organometallics* **2014**, *33*, 5952 – 5955.
[21] R. F. Koby, T. P. Hanusa, N. D. Schley, *J. Am. Chem. Soc.* **2018**, *140*, 15934 – 15942.
[22] I. R. Speight, S. C. Chmely, T. P. Hanusa, A. L. Rheingold, *Chem. Commun.* **2019**, *55*, 2202 – 2205.
[23] Superficially, the splitting pattern and ratio of intensities would suggest a compound with 3*n* (η^3-A′) ligands. In fact, as is typical for allylmagnesium complexes, the compound is fluxional in solution. Cooling a sample even slightly (253 K) reveals new resonances in the ^{1}H NMR spectrum in tol-d_8, the most obvious of which are an apparent triplet at δ6.72 ($J = 16$ Hz), accompanied by a new doublet at δ2.89. Despite the complexity of the spectrum, there is no evidence for dissociation into [{MgA'_2}$_2$] and K[A′], that is, the aggregate appears to remain intact. See the Supporting Information for additional details.
[24] L. K. Engerer, C. N. Carlson, T. P. Hanusa, W. W. Brennessel, J. V. G. Young, *Organometallics* **2012**, *31*, 6131 – 6138.
[25] U. Schümann, E. Weiss, H. Dietrich, W. Mahdi, *J. Organomet. Chem.* **1987**, *322*, 299 – 307.
[26] C. K. Gren, T. P. Hanusa, A. L. Rheingold, *Main Group Chem.* **2009**, *8*, 225 – 235.
[27] a) K. T. Quisenberry, C. K. Gren, R. E. White, T. P. Hanusa, W. W. Brennessel, *Organometallics* **2007**, *26*, 4354 – 4356; b) C. K. Simpson, R. E. White, C. N. Carlson, D. A. Wrobleski, C. J. Kuehl, T. A. Croce, I. M. Steele, B. L. Scott, T. P. Hanusa, A. P. Sattelberger, K. D. John, *Organometallics* **2005**, *24*, 3685 – 3691; c) T. J. Woodman, M. Schormann, D. L. Hughes, M. Bochmann, *Organometallics* **2004**, *23*, 2972 – 2979.
[28] a) A. Parry in *Reactivity, Mechanism and Structure in Polymer Chemistry* (Eds.: A. D. Jenkins, A. Ledwith), Wiley, London, **1974**, pp. 350 – 382; b) Y. Li, H. Deng, W. Brittain, M. S. Chisholm, *Polym. Bull.* **1999**, *42*, 635 – 639; c) S.-L. Zhou, S.-W. Wang, G.-S. Yang, X.-Y. Liu, E.-H. Sheng, K.-H. Zhang, L. Cheng, Z.-X. Huang, *Polyhedron* **2003**, *22*, 1019 – 1024; d) L. S. Boffa, B. M. Novak, *Transition Metal Catalysis in Macromoloecular Design*, Oxford University Press, Washington, **2000**.
[29] a) C. K. Gren, T. P. Hanusa, A. L. Rheingold, *Organometallics* **2007**, *26*, 1643 – 1649; b) A. S. Reddy, H. Zipse, G. N. Sastry, *J. Phys. Chem. B* **2007**, *111*, 11546 – 11553.
[30] R. A. Layfield, F. García, J. Hannauer, S. M. Humphrey, *Chem. Commun.* **2007**, 5081 – 5083.
[31] R. D. Shannon, *Acta Crystallogr. Sect. A* **1976**, *32*, 751 – 767.
[32] A. L. Allred, *J. Inorg. Nucl. Chem.* **1961**, *17*, 215 – 221.
[33] C. Lichtenberg, J. Engel, T. P. Spaniol, U. Englert, G. Raabe, J. Okuda, *J. Am. Chem. Soc.* **2012**, *134*, 9805 – 9811.
[34] a) K. M. Krebs, J. Wiederkehr, J. Schneider, H. Schubert, K. Eichele, L. Wesemann, *Angew. Chem. Int. Ed.* **2015**, *54*, 5502 – 5506; *Angew. Chem.* **2015**, *127*, 5593 – 5597; b) A local minimum for [SnA'_2] with η^3-bound ligands could not be located at the B3PW91-D3BJ/def2TZVP level, even under imposed C_2 symmetry.
[35] To maintain η^1-bound ligands, both [BeA'_2] and [MgA'_2] had to be optimized under C_i symmetry. The σ-bound forms possessed imaginary frequencies, with the largest for [MgA'_2] at -31 cm^{-1}.
[36] R. F. Koby, N. R. Rightmire, N. D. Schley, T. P. Hanusa, W. W. Brennessel, *Beilstein J. Org. Chem.* **2019**, *15*, 1856 – 1863.
[37] I. A. Guzei, M. Wendt, *Dalton Trans.* **2006**, 3991 – 3999.
[38] The coordination environment in **1** was defined as a sphere of 7.6 Å radius around Mg1. This incorporates three complete allyl ligands directly bonded to the Mg and two potassium cations.
[39] C. Elschenbroich, *Organometallics*, 3rd. ed., VCH Publishers, Weinheim, **2006**, p. 440.
[40] N. Takagi, M. W. Schmidt, S. Nagase, *Organometallics* **2001**, *20*, 1646 – 1651.
[41] a) A. J. Martinez-Martinez, C. T. O'Hara, in *Advances in Organometallic Chemistry*, *Vol. 65* (Ed.: P. J. Perez), Elsevier, Amsterdam, **2016**, pp. 1 – 46; b) S. D. Robertson, M. Uzelac, R. E. Mulvey, *Chem. Rev.* **2019**, *119*, 8332 – 8405.
[42] CCDC 1972897 contains the supplementary crystallographic data for this paper. These data are provided free of charge by The Cambridge Crystallographic Data Centre.

Manuskript erhalten: 21. Dezember 2019
Veränderte Fassung erhalten: 7. Februar 2020
Akzeptierte Fassung online: 11. Februar 2020
Endgültige Fassung online: 1. April 2020

